The American Journal of Pathology, Vol. 193, No. 9, September 2023

ELSEVIER

The American Journal of PATHOLOGY

ajp.amjpathol.org

CARDIOVASCULAR, PULMONARY, AND RENAL PATHOLOGY

Dickkopf1 Promotes Pulmonary Fibrosis upon Bleomycin-Induced Lung Injury

Eun-Ah Sung,*† Min Hee Park,*† Octavian Henegariu,‡ Patricia J. Sime,*§ and Wook-Jin Chae*†

From the Departments of Microbiology and Immunology and Internal Medicine,§ and the Massey Cancer Center,† Virginia Commonwealth University School of Medicine, Richmond, Virginia; and the Department of Neurosurgery,‡ Yale University School of Medicine, New Haven, Connecticut*

Accepted for publication May 19, 2023.

Address correspondence to Wook-Jin Chae, Ph.D., Department of Microbiology and Immunology, Virginia Commonwealth University, GRL-282, 401 College St., Richmond, VA 23298. E-mail: wook-jin.chae@vcuhealth.org.

Orchestration of inflammation and tissue repair processes is critical to maintaining homeostasis upon tissue injury. Tissue fibrosis is a pathological process characterized by aberrant accumulation of extracellular matrix proteins, such as collagen, upon injury. Dickkopf1 (DKK1) is a quintessential Wnt antagonist. The role of DKK1 in bleomycin (BLM)-induced lung injury and fibrosis model remains elusive. This study shows that BLM-induced lung injury markedly elevated DKK1 protein expressions in the lungs in mice, consistent with human pulmonary fibrosis patient lung tissues. The elevated DKK1 levels coincided with immune cell infiltration and collagen deposition. Notably, the reduced expression of DKK1 in Dkk1 hypomorphic *doubleridge* (*Dkk1*$^{d/d}$) mice abrogated BLM-induced lung inflammation and fibrosis. Immune cell infiltration, collagen deposition, expression of profibrotic cytokine transforming growth factor β1 (TGF-β1), and extracellular matrix protein–producing myofibroblast marker α-smooth muscle actin (α-SMA) were reduced in *Dkk1*$^{d/d}$ mice. Consistent with these results, local DKK1 antibody administration after BLM-induced lung injury substantially decreased lung inflammation and fibrosis phenotypes. Taken together, these results demonstrate that DKK1 is a proinflammatory and profibrotic ligand that promotes inflammation and fibrosis upon BLM-induced lung injury, placing it as an attractive molecular target for dysregulated pulmonary inflammation and tissue repair. *(Am J Pathol 2023, 193: 1130–1142; https://doi.org/10.1016/j.ajpath.2023.05.009)*

The human body encounters a myriad of environmental challenges, including infection and sterile injuries.[1] Maintaining tissue homeostasis upon these injuries requires orchestrating multistep processes that consist of inflammation, fibroproliferation, and tissue remodeling and regeneration.[2]

The Wnt signaling regulates cell proliferation and differentiation and is important for tissue repair and remodeling.[3] Dysregulation of the canonical Wnt pathway mediators and ligands has been reported in various diseases such as cancer.[4] Dickkopf1 (DKK1) is a Wnt antagonistic ligand that binds to its receptor, low-density lipoprotein receptor-related protein 6 (LRP6). Although the role of DKK1 as a Wnt antagonist has been well-established, recent studies have revealed that DKK1 expression is elevated at local and systemic levels in mice and humans in pathological and chronic inflammatory diseases.[5–7] Additionally, DKK1's function as a proinflammatory immunomodulator in type 2 and type 17 inflammation has been demonstrated.[8,9]

The lungs are uniquely positioned to meet myriad environmental challenges, and thus require fine-tuning of immune responses and tissue repair processes.[10] Pulmonary fibrosis (PF) is a progressive fibroproliferative disease caused by uncontrolled injury–inflammation–repair processes with the excessive deposition of an extracellular matrix protein, such as collagen. After PF diagnosis, the median survival time is

Supported by the Massey Cancer Center Harrison Scholar Fund (W.-J.C.), Cancer Cell Signaling Leadership program award (W.-J.C.), Virginia Commonwealth University (VCU) fund (W.-J.C.), VCU's National Center for Advancing Translational Science grant UL1TR002649, and the VCU Center for Clinical and Translational Research Endowment Fund (W.-J.C.), and in part by American Cancer Society grant IRG-18-159-43 (W.-J.C.). Histology services for this research were generated by the VCU Cancer Mouse Models Core Laboratory, supported, in part, by NIH-NCI Cancer Center Support grant P30 CA016059.

Disclosures: None declared.

https://doi.org/10.1016/j.ajpath.2023.05.009

approximately 3 years.[11] Effective therapeutic methods remain an urgent and unmet medical need.[12] Thus, a better understanding of the molecular and cellular mechanisms of PF is crucial for the therapeutic approach.

The bleomycin (BLM)-induced lung injury model is one of the most widely used mouse models for PF. BLM-mediated lung injury promotes lung inflammation and fibrosis.[13,14] BLM is a profibrotic agent causing PF when intravenously administered for lymphoma treatment.[15] The BLM-induced lung fibrosis in mice is similar to the accelerated acute phase of PF in humans.[16] The elevated levels of DKK1 in human PF patients and Wnt3a in BLM-induced lung fibrosis in mice have been reported.[17,18] Whether the elevated DKK1 protein levels cause PF pathology remains elusive.

Transforming growth factor β1 (TGF-β1) plays an essential role as a key profibrotic cytokine to promote pulmonary fibrosis.[2,19] TGF-β1 induces α-smooth muscle actin (α-SMA)$^+$ myofibroblast differentiation and activation, producing extracellular matrix proteins to provide the necessary mechanical properties to facilitate the particular function of the organ.[20] Several studies demonstrated that the excessive profibrotic cytokine TGF-β1 and dysregulated inflammation promote PF.[21–23] PF is characterized by excessive proliferation of myofibroblasts by increased profibrotic cytokines and accumulation of extracellular matrix components. This disorder causes disrupted tissue architecture and leads to major impairments in organ function.[24,25]

This study addressed the role of DKK1 using the BLM-induced lung inflammation and fibrosis model. DKK1 protein levels substantially increased in both human PF lung tissues and the lungs from the BLM-induced lung injury model in mouse. *Dkk1* hypomorphic *doubleridge* mice markedly reduced BLM-induced lung inflammation and fibrosis. Local DKK1 antibody treatment after BLM challenge showed that DKK1 neutralization can be an effective therapeutic target in PF.

Materials and Methods

Mice

C57Bl/6J mice (#000664) were purchased from the Jackson Laboratory (Bar Harbor, ME) and have been bred in the authors' mouse facility. *Dkk1* hypomorphic *doubleridge* (*Dkk1*$^{d/d}$) mice were kindly provided by Dr. Asma Nusrat (Emory University) and described previously.[8] All mouse protocols were approved by the VCU Animal Care and Use Committee approval in accordance with the Association for Assessment and Accreditation of Laboratory Animal Care International.

The Bleomycin-Induced Lung Injury Model

BLM (bleomycin sulfate, S121415; Selleckchem, Houston, TX), 4 U/kg, was dissolved in 40 μL of PBS for each mouse per intranasal challenge. Eight- to 10-week–old *Dkk1*$^{d/d}$ mice and their littermate controls were challenged with BLM intranasally on day 0. Mice were sacrificed, and lungs were harvested on day 14. DKK1 antibody (DKK1 Ab) (Amgen, Thousand Oaks, CA) and isotype rat IgG (Sigma-Aldrich, Saint Louis, MO) were used. After lung perfusion, lungs were fixed with 10% formalin (23-245685; Fisher Scientific, Waltham, MA) for at least 48 hours and embedded in paraffin for histological analysis and formalin-fixed paraffin-embedded (FFPE) quantitative PCR (qPCR). Paraffin sections were prepared by microtome (HM355S1; Microm, Hessen, Germany).

Immunohistochemistry

Lung tissue sections (5 μm thick) were deparaffinized with Histoclear (H2779; Sigma-Aldrich) and then dehydrated. Sodium citrate buffer (10 mmol/L, pH 6.0) was used for antigen retrieval. Endogenous peroxidases were blocked using 3% H_2O_2. The sections were incubated with 5% bovine serum albumin and subsequently stained with primary antibodies. The sections were stained with 5 μg/mL of the secondary antibody. For DKK1, the ABC reagent (PK-7100; Vector Laboratories, Newark, CA) was added. Sections were developed using a DAB substrate kit (SK-4100; Vector Laboratories). Counterstaining was performed using Mayer's hematoxylin (MHS32; Sigma-Aldrich). The sections were mounted with a mounting solution (H-5000; Vector Laboratories). Images were acquired using the Vectra Polaris system (Akoya Biosciences, Marlborough, MA).

A human lung tissue array (pulmonary interstitial fibrosis tissue array, LC561; Biomax, Derwood, MD) was purchased. The sections were prepared with the same methods as mouse lung tissue sections. Images were acquired using the Vectra Polaris. Primary and secondary antibody details are shown in Table 1.

Masson's Trichrome Staining

Lung tissue sections (5 μm thick) were deparaffinized with Histoclear and dehydrated using ethanol. The sections were post-fixed in Bouin's Solution (11750-32; IHC World, Woodstock, MD). They were stained with Masson Trichrome Stain Kit (IW-3006; IHC World) according to the manufacturer's protocol. The sections were mounted with the mounting solution (H-5000; Vector Laboratories). Images were acquired using the Vectra Polaris (Akoya Biosciences).

Hematoxylin and Eosin Staining

For histological analysis, lung tissue sections (5 μm thick) were used. The nuclei were stained by hematoxylin for 3 minutes at room temperature. The cytoplasm was stained by eosin (HT110132; Sigma-Aldrich). The sections were

mounted with the mounting solution (H-5000; Vector Laboratories), and images were acquired using the Vectra Polaris (Akoya Biosciences).

Quantification of Immunohistochemistry Images

Images were saved as TIFF files using Phenochart, a slider viewer software (version 1.1.0, Akoya Biosciences). Images were processed using the Color Deconvolution plugin with a specific type of staining selection in Fiji software version 2.9.0/1.53t (*https://imagej.net/software/fiji*) (H DAB stain for DKK1, α-SMA and TGF-β1 IHC, Masson trichrome for Masson's trichrome staining). Images were deconvoluted in their color components. The brown component of H DAB and the green component of Masson trichrome was measured using the Threshold tool. The threshold value of the deconvoluted images was adjusted, and the same value of the threshold was applied to all processed images. The selected area of the image was analyzed using the Measure tool. Total DKK1, α-SMA, and TGF-β1 protein expressions and total collagen deposition were quantified from the entire tissue section. For parenchyma collagen deposition, pictures from 10 fields were randomly taken in the alveolar region of the lungs to exclude big bronchi/arterial structures and then quantified.

RNA Isolation from FFPE Tissue

From FFPE lung tissues, 20-μm-thick lung tissue sections were used. Two lung tissue sections per paraffin block were deparaffinized by adding Histoclear and used for the RNeasy FFPE kit (73504; QIAGEN, Germantown, MD). After deparaffinization, RNA was extracted by RNeasy FFPE kit according to the manufacturer's protocol.

Real-Time qPCR

Reverse transcription of total RNA was performed using RNA to cDNA EcoDry Premix kit (639548; Takara Bio, San Jose, CA). qPCR was performed using PowerUp SYBR Green Master Mix (A25742; Thermo Fisher Scientific, Waltham, MA). The reaction was detected on a QuantStudio 3 or 5 Flex Real-Time PCR system (Thermo Fisher Scientific). The mRNA levels of target genes were normalized by comparing them to the mRNA level of β-actin or Gapdh controls using the $2^{-\Delta\Delta C_T}$ method.

Table 1 Information on Primary and Secondary Antibodies

Antibody	Manufacturer	Catalog no.
Goat polyclonal anti-m/hDKK1	R&D Systems	AF1096
Rabbit polyclonal anti—α-SMA	Thermo Fisher Scientific	PA5-16697
Rabbit polyclonal anti—TGF-β1	Proteintech	21898-1-AP
Normal goat IgG	R&D Systems	AB-108-C
Biotinylated rabbit anti-goat IgG	Vector Laboratories	BA-5000
HRP-conjugated mouse anti-goat IgG	Santa Cruz Biotechnology	sc-2354
HRP-conjugated mouse anti-rabbit IgG	Santa Cruz Biotechnology	sc-2357

Flow Cytometry

After mouse lung perfusion, single-cell lung homogenates were prepared by collagenase digestion (280 U/mL collagenase type IV; Worthington Biochemicals, Lakewood, NJ), 2% (v/v) fetal bovine serum (Gemini Bio-Products, West Sacramento, CA), and 40 μg/mL DNase I (Roche, Indianapolis, IN) in sterile PBS using the gentleMACS Octo Dissociator (Miltenyi Biotec, Auburn, CA).

After blocking Fc receptor, cells were stained with Zombie Aqua Fixable Viability Kit (423102; BioLegend, San Diego, CA). Subsequently, the cells were stained with fluorescent-conjugated antibodies against different cell surface antigens or isotype control. Following surface staining, cells were fixed with IC Fixation Buffer (00-8333; Thermo Fisher Scientific). Detailed information on the used antibodies is described in Table 2. The FACSCanto system (BD Biosciences, Franklin Lakes, NJ) was used for flow cytometry, and data were analyzed by FlowJo software version 10.7 (Ashland, OR).

Western Blot

Lung homogenate lysates were separated by SDS-PAGE and transferred onto a polyvinylidene difluoride membrane. The membrane was blocked and immunoblotted with primary antibodies against DKK1 (AF1096; R&D systems, Minneapolis, MN) at 1:1500 dilution and β-actin (3700; Cell Signaling, Danvers, MA) at 1:5000 dilution. After washing with TBS-T, the membrane was incubated with horseradish peroxidase—conjugated secondary antibodies for 1 hour at room temperature. The membrane was developed using a WesternBright Sirius kit (K-12043-D10; Advansta, San Jose, CA). Bands were detected and quantified using the Chemidoc and ImageJ software version 1.52t (NIH, Bethesda, MD; *http://imagej.nih.gov/ij*) and normalized to β-actin protein levels.

Enzyme-Linked Immunosorbent Assay

The mouse DKK1 enzyme-linked immunosorbent assay kit was purchased from R&D systems (MKK100). Concentrations of circulating DKK1 in plasma samples were measured by enzyme-linked immunosorbent assay according to the manufacturer's protocol.

Table 2 Information on Antibodies

Antibody	Manufacturer	Catalog no.
APC/Fire 750 anti-mouse CD45, clone 30-F11	BioLegend	103154
APC mouse IgG1 kappa isotype ctrl antibody, clone MOPC-21	BD Biosciences	550854
Biotin anti-mouse Ly-6G, clone 1A8	BioLegend	127603
eFluor 660 anti-mouse CD170 (Siglec F), clone 1RNM44N	eBioscience	50-1702-80
eFluor 450 streptavidin	eBioscience	48-4317-82
FITC anti-mouse CD4, clone RM4-5	BioLegend	100510
FITC mouse IgG1 kappa isotype ctrl antibody, clone MOPC-21	BioLegend	400107
Pacific Blue anti-mouse TCR beta chain, clone H57-597	BioLegend	109226
Pacific Blue rat IgG2α kappa isotype ctrl antibody, clone RTK2758	BioLegend	400527
PE mouse IgG1 kappa isotype ctrl antibody, clone P3.6.2.8.1	eBioscience	12-4714-82
PE streptavidin	BioLegend	405204
PerCP/Cyanine5.5 anti-mouse CD64 (FcγRI), clone X54-5/7.1	BioLegend	139308
PerCP/Cyanine5.5 anti-mouse CD8b.2, clone 53-5.8	BioLegend	140417
PerCP/Cyanine5.5 rat IgG2a kappa isotype ctrl antibody, clone RTK2758	BioLegend	400531
PE/Cyanine7 anti-mouse CD11c, clone N418	BioLegend	117317
PE/Cyanine7 anti-mouse NK1.1, clone PK136	BioLegend	108714
PE/Cyanine7 mouse IgG1 kappa isotype ctrl antibody, clone MOPC-21	BioLegend	400125
Ultra-LEAF purified anti-mouse CD16/32 antibody	BioLegend	101330

Hydroxyproline Quantitation Assay

Lungs were harvested and processed for quantitation of hydroxyproline using a hydroxyproline assay kit (MAK008; Sigma-Aldrich). Hydroxyproline concentration was measured by colorimetric assay (560 nm) based on the manufacturer's protocol.

Statistical Analysis

Statistically significant differences were analyzed by *t*-test, one-way analysis of variance analysis with Bonferroni's post hoc test with GraphPad Prism software version 9.4.1 (GraphPad Software Inc., San Diego, CA).

Results

DKK1 Protein Levels Are Increased in the Murine Bleomycin-Induced Lung Injury Model and Human Pulmonary Fibrosis Tissues

The study tested whether DKK1 protein levels are elevated in various PF patient lung tissues. The lung tissue microarray from human PF patients was used for DKK1 immunohistochemistry (IHC) staining. Lung tissues from PF patients ($n = 9$) showed markedly increased DKK1 protein levels (2.9-fold) compared with those from healthy controls ($n = 7$) (Figure 1A and Supplemental Table S1). This prompted investigation into whether DKK1 promotes lung fibrosis phenotype in the BLM-induced lung injury model in mice.

Two weeks after a BLM challenge, local DKK1 protein levels in the lung were elevated about 2.5-fold (Figure 1B), as indicated by Western blot. The systemic levels of circulating DKK1 in plasma were also elevated, suggesting that the BLM challenge induced a systemic increase in DKK1 levels (Figure 1C). The increase of DKK1 protein levels in the lung upon BLM challenge was quantitated using DKK1 IHC images (Figure 1D). DKK1 IHC showed that DKK1 protein levels in the right lung lobe were increased by 1.85-fold in BLM-treated mice compared with control mice. Time kinetics of DKK1 in the lung were investigated upon BLM challenge. DKK1 protein levels in the lung were steadily elevated till day 14 after a single BLM challenge (Supplemental Figure S1). The results demonstrated that DKK1 protein levels are elevated in both PF patients and BLM-challenged mice.

Reduced Expression of DKK1 in *Doubleridge* Mice Abrogates BLM-Induced Lung Inflammation

To explore whether the reduced DKK1 expression protects mice from BLM-induced lung inflammation, *Dkk1* hypomorphic *doubleridge* ($Dkk1^{d/d}$) mice were used. $Dkk1^{d/d}$ mice have 90% reduced DKK1 expression with normal immunological phenotypes in the spleen and peripheral blood.[8,26] Previously, *doubleridge* mice and their littermate control (LC) mice showed little difference in immune cell populations in the spleen. Consistently, no notable differences were observed in immune cell infiltration and populations between vehicle-treated $Dkk1^{d/d}$ mice and LC mice lungs. These results indicated that the reduced DKK1 protein expression did not alter baseline immune cell profiles in the lung (Figure 2).

Hematoxylin & eosin (H&E) staining using the lungs from LC mice that were challenged with BLM intranasally showed increased inflammation and leukocyte infiltration (Figure 2A). Inflammation and leukocyte infiltration were substantially reduced in BLM-treated $Dkk1^{d/d}$ mice compared with BLM-treated LC mice by H&E staining

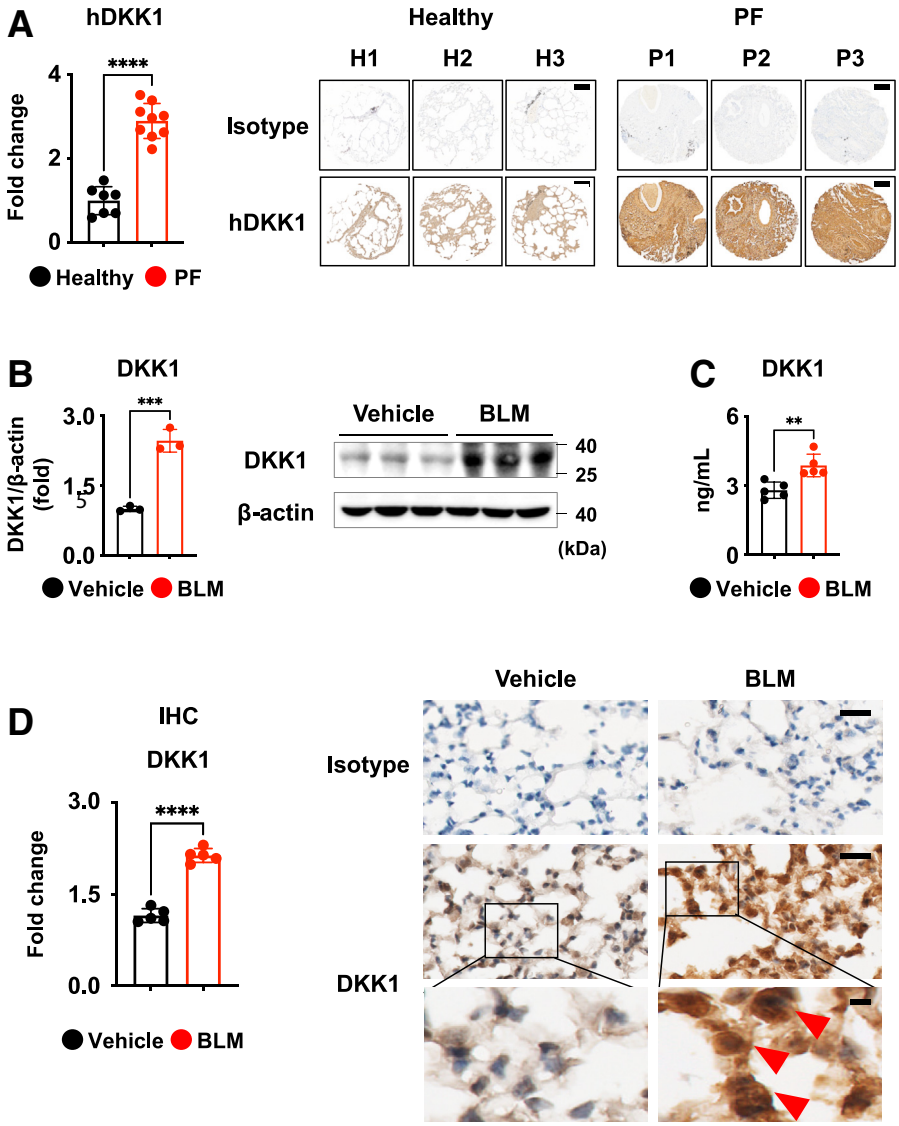

Figure 1 Human PF patient lung tissues and mouse lungs from the bleomycin (BLM)-induced lung fibrosis model show elevated DKK1 protein levels. **A:** Human lung tissue microarrays from healthy donors (Healthy) and pulmonary fibrosis patients (PF) were analyzed for human DKK1 (hDKK1) by immunohistochemistry (IHC) and quantified using ImageJ software version 1.52t (**left**). Representative images of IHC are shown (**right**). **B**–**D:** C57Bl/6J mice were challenged with BLM intranasally on day 0. Controls were challenged with PBS (vehicle). On day 14, the lungs and peripheral blood were collected. **B:** The ratio of DKK1 to β-actin was quantified by Western blot and ImageJ. **C:** Circulating DKK1 protein levels were determined by DKK1 ELISA enzyme-linked immunosorbent assay. **D:** Total DKK1 protein levels were analyzed by IHC and ImageJ software (**left**). Representative images of IHC are shown (**right**). The **boxed areas** are shown in higher magnification below. DKK1-positive cells are indicated by **arrowheads**. A representative of two independent experiments is shown. Data are expressed as means ± SD. $n = 7$ healthy donors (**A**); $n = 9$ PF patients (**A**); $n = 3$ per group (**B**); $n = 5$ per group (**C** and **D**). $^{**}P < 0.005$ $^{***}P < 0.001$, and $^{****}P < 0.0001$ (*t*-test). Scale bars: 300 μm (**A**); 20 μm (**D**, **top** and **middle panels**); 5 μm (**D**, **bottom panels**). Original magnification: ×60 (**D**, **top** and **middle panels**); ×80 (**D**, **bottom panels**).

(Figure 2A). Total leukocytes ($CD45^+$), macrophages, neutrophils, eosinophils, $CD4^+$ T cells, $CD8^+$ T cells, and natural killer (NK) cells from lung tissue homogenates were quantitated by flow cytometry (Supplemental Figure S2). Consistent with the result from H&E staining, leukocyte ($CD45^+$) infiltration was substantially decreased in *Dkk1*$^{d/d}$ mice compared with LC mice upon BLM challenge (a 46% decrease) (Figure 2B). The increased numbers of myeloid lineage cells (eg, macrophages, neutrophils, and eosinophils), T cells, and NK cells upon BLM injury were significantly abolished in *Dkk1*$^{d/d}$ mice compared with LC mice in the lung (Figure 2B). These results demonstrated that the reduced expression of DKK1 protein in *Dkk1*$^{d/d}$ mice abrogated lung inflammation upon BLM challenge.

Reduced Expression of DKK1 in *Doubleridge* Mice Abolishes BLM-Induced Lung Fibrosis Phenotypes

Whether BLM-induced lung fibrosis phenotypes were decreased in *Dkk1*$^{d/d}$ mice was investigated next. *Dkk1*$^{d/d}$ and LC mice were examined for DKK1 protein levels in the lung upon BLM challenge. BLM-treated *Dkk1*$^{d/d}$ mice showed

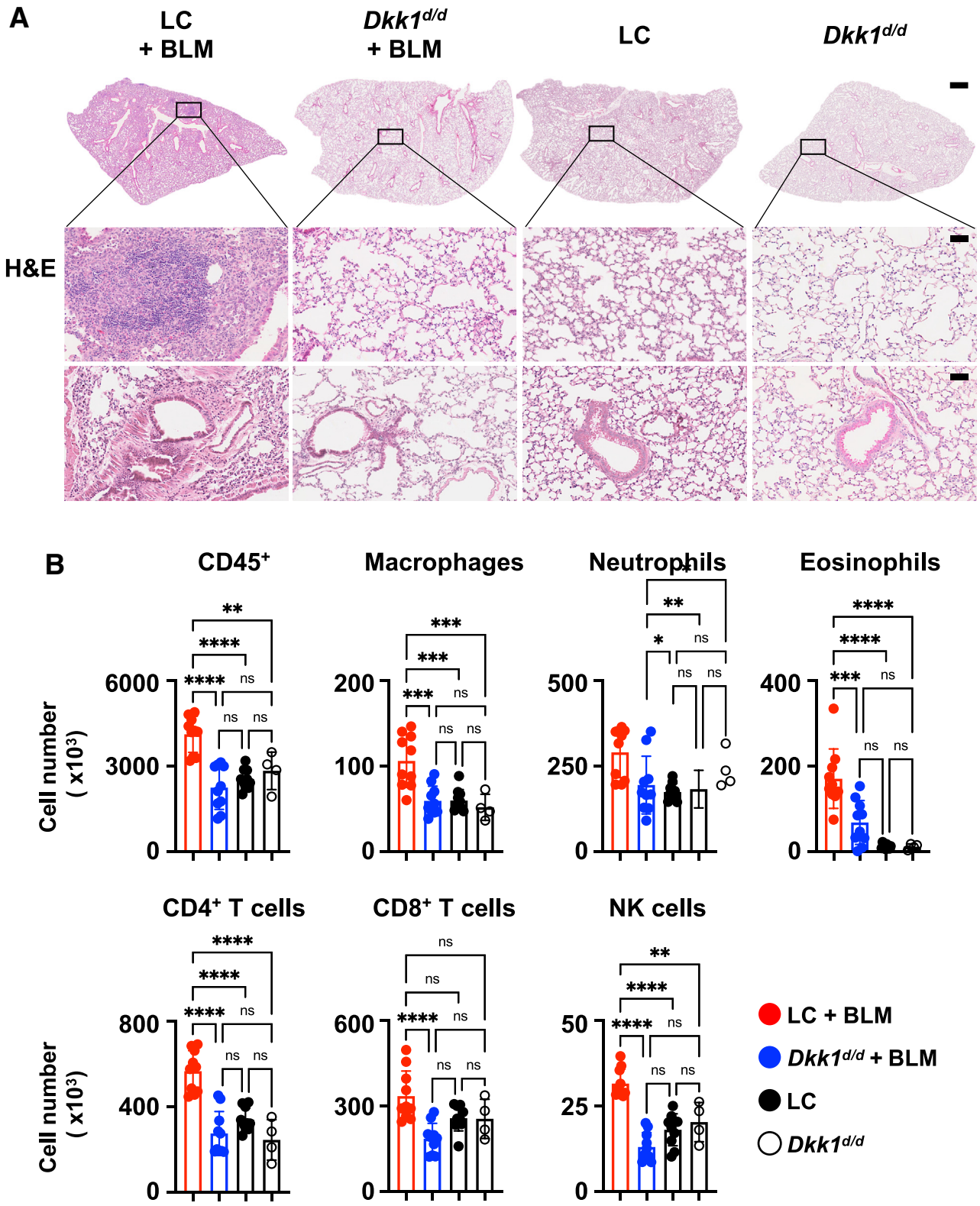

Figure 2 *Doubleridge* mice show reduced bleomycin (BLM)-induced lung inflammation. **A** and **B:** *Dkk1*$^{d/d}$ mice and their wild-type littermate controls (LC) were challenged with BLM. On day 14, the lungs were harvested. **A:** Representative images of hematoxylin & eosin (H&E) staining are shown. The **boxed areas** are shown in higher magnification below. **B:** Total leukocytes (CD45^{+}), macrophages, neutrophils, eosinophils, CD4^{+} T cells, CD8^{+} T cells, and NK cells from lung tissue homogenates were quantitated by flow cytometry. A representative of two independent experiments is shown. Data are expressed as means ± SD. $n = 10$ per LC + BLM, *Dkk1*$^{d/d}$ + BLM, and LC group (**B**); $n = 4$ per *Dkk1*$^{d/d}$ group (**B**). $^{*}P < 0.05$, $^{**}P < 0.005$, $^{***}P < 0.001$, and $^{****}P < 0.0001$ (one-way analysis of variance analyses with Bonferroni's post hoc test). Scale bars: 800 μm (**A**, **top panels**); 50 μm (**A**, **middle** and **bottom panels**). Original magnification: ×1 (**A**, **top panels**); ×10 (**A**, **middle** and **bottom panels**). ns, not significant.

minimal DKK1 protein levels, close to the levels of vehicle-treated LC and *Dkk1*$^{d/d}$ mice (Figure 3A).

Dkk1$^{d/d}$ mice showed a significant decrease in Col1a1 mRNA expression compared with LC mice 2 weeks after a BLM challenge (a 36% decrease) (Figure 3B). Masson's trichrome staining of lung tissues was used to detect collagen deposition. Consistent with the Col1a1 mRNA result, BLM-treated LC mice showed a marked increase in collagen deposition at the sites surrounding vascular vessels or bronchioles and in the parenchyma area compared with vehicle-treated LC mice (a 60% increase) (Figure 3, C and D). Notably, *Dkk1*$^{d/d}$ mice had very little collagen deposition upon BLM-induced lung injury compared with LC mice, indicating that DKK1 is required for collagen deposition (Figure 3, C and D). The whole lung area of Masson's trichrome–stained images was quantified. The collagen-positive areas in the whole lung were decreased by 30% in *Dkk1*$^{d/d}$ mice compared with LC mice (Figure 3, C and D). Consistent with these findings, hydroxyproline concentration in the *Dkk1*$^{d/d}$ mice lungs was decreased compared with LC mice upon BLM challenge (Supplemental Figure S3). In PF, excessive collagen deposition in the lung parenchyma area causes the destruction of normal lung physiology.[27] Herein, parenchyma collagen deposition was examined using Masson's trichrome–stained images. Ten fields were randomly selected in the parenchyma region of the lungs, excluding big bronchiole and arterial structures, to detect parenchyma collagen deposition.[28] The decrease of collagen-positive areas became more prominent (a 70% decrease) in *Dkk1*$^{d/d}$ mice in the lung parenchyma (Figure 3, C and D) as compared to those in LC lungs. There were no significant differences in Col1a1 mRNA expression and collagen deposition between vehicle-treated *Dkk1*$^{d/d}$ mice and LC mice lungs (Figure 3, B, C, and D).

Next, myofibroblast marker α-SMA and profibrotic cytokine TGF-β1 protein levels were determined in *Dkk1*$^{d/d}$ and LC mice after the BLM challenge. The α-SMA and TGF-β1 protein levels in the lung upon BLM challenge

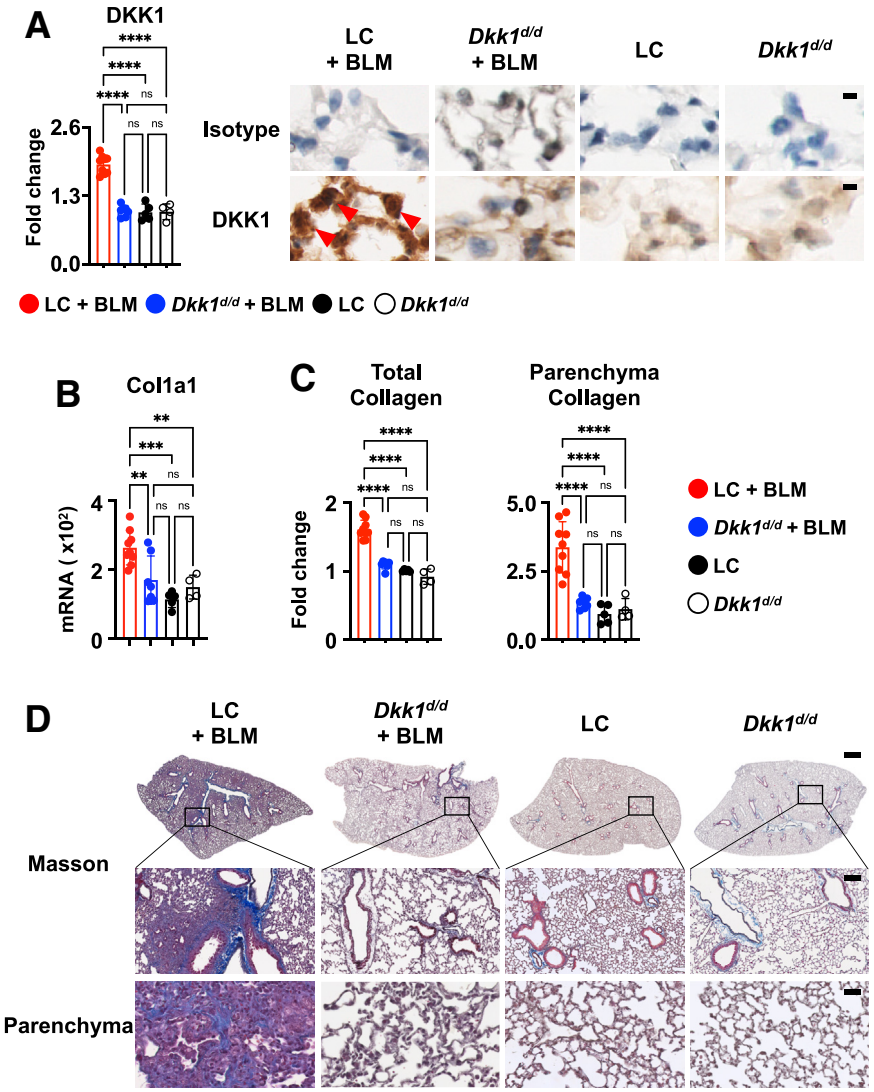

Figure 3 *Doubleridge* mice show reduced collagen deposition upon bleomycin (BLM) challenge. **A**–**C:** *Dkk1*$^{d/d}$ mice and littermate control (LC) mice were challenged with BLM. On day 14, the lungs were harvested. **A:** DKK1 protein levels were analyzed by immunohistochemistry, and ImageJ software version 1.52t (**left**). Representative images of immunohistochemistry are shown (**right**). DKK1-positive cells are indicated by **arrowheads**. **B:** Lung tissue sections were analyzed by formalin-fixed paraffin-embedded quantitative PCR. Relative Col1a1 gene expression levels were quantitated. **C:** Total collagen and parenchyma collagen depositions were determined by Masson staining and ImageJ software. **D:** Representative images of Masson staining are shown. The **boxed areas** are shown in higher magnification below. A representative of two independent experiments is shown. Data are expressed as means ± SD. $n = 9$ per LC + BLM group (**A**–**C**); $n = 7$ per *Dkk1*$^{d/d}$ + BLM group (**A**–**C**); $n = 5$ per LC group (**A**–**C**); $n = 4$ per *Dkk1*$^{d/d}$ group (**A**–**C**). $^{**}P < 0.005$, $^{***}P < 0.001$, and $^{****}P < 0.0001$ (one-way analysis of variance analyses with Bonferroni's post hoc test). Scale bars: 5 μm (**A**); 800 μm (**D**, **top panels**); 100 μm, (**D**, **middle panels**); 20 μm (**D**, **bottom panels**). Original magnification: ×80 (**A**);×1 (**D**, **top panels**); ×10 (**D**, **middle panels**); ×40 (**D**, **bottom panels**). ns, not significant.

were quantitated using IHC images of lung tissues. BLM-treated LC mice showed increased α-SMA protein levels (Figure 4, A and C). IHC image quantification showed marked decreases in α-SMA protein levels in *Dkk1*$^{d/d}$ mice lungs compared with LC mice upon BLM-induced lung injury (a 48% decrease) (Figure 4, A and C). Consistent with these findings, TGF-β1 protein levels were markedly decreased in the BLM-treated *Dkk1*$^{d/d}$ mice lungs compared with BLM-treated LC mice (a 34% decrease) (Figure 4, B, and C). Vehicle-treated *Dkk1*$^{d/d}$ mice and LC mice did not show any significant differences in α-SMA and TGF-β1 protein levels (Figure 4, A-C). The results suggest that the reduced expression of DKK1 in *Dkk1*$^{d/d}$ mice abrogates key fibrotic cellular events such as collagen deposition, myofibroblast activation, and increased profibrotic cytokine TGF-β1 expression, protecting mice from lung fibrosis phenotype upon BLM injury.

Neutralization of DKK1 in BLM-Induced Lung Injury Inhibits Pulmonary Fibrosis Phenotypes

Given that *Dkk1*$^{d/d}$ mice showed reduced lung fibrosis phenotypes, DKK1 neutralization as a therapeutic approach was tested in the BLM-induced lung inflammation and fibrosis. It has been suggested that the fibrotic phase of BLM-induced fibrosis starts 1 week after the initial injury.[29] Anti-DKK1 Ab or isotype Ab was treated intranasally either through full treatment (week 1 and 2) or late treatment protocol (week 2 only) (Figure 5A). In the full treatment protocol, DKK1 Ab or isotype Ab was treated 1 day before

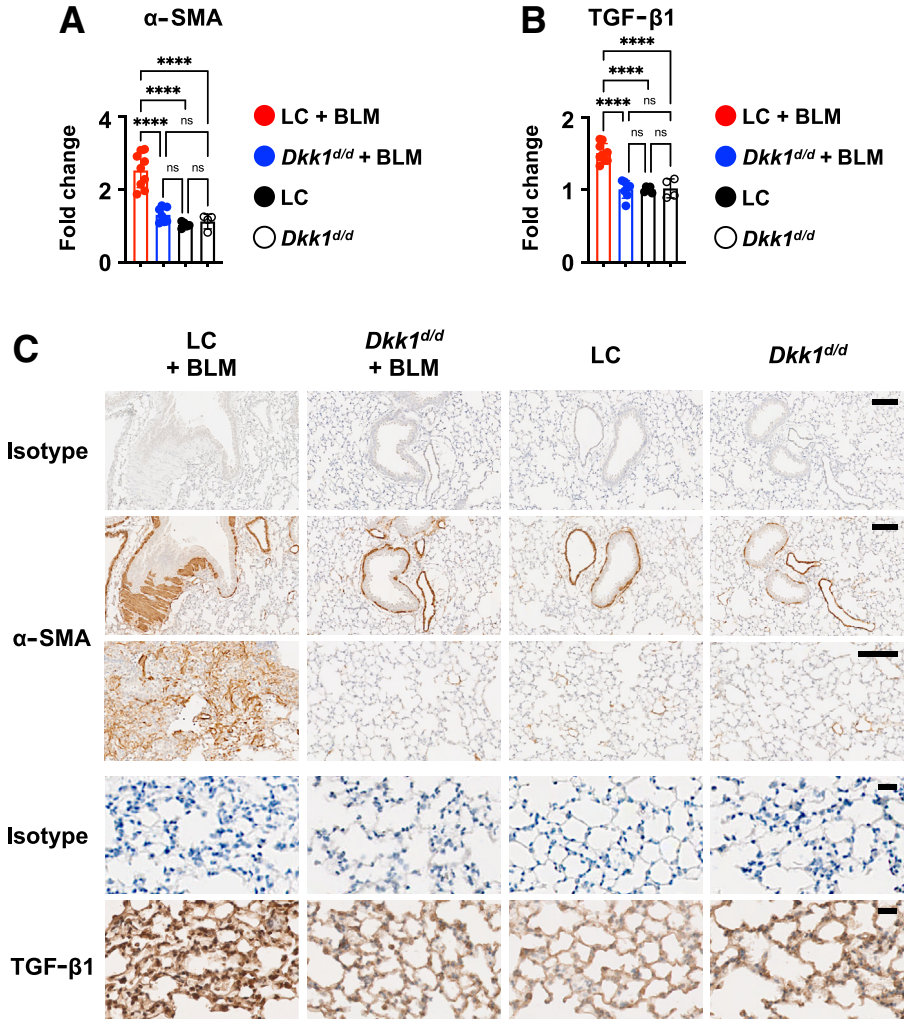

Figure 4 Doubleridge mice show reduced bleomycin (BLM)-induced lung fibrosis phenotypes. **A** and **B:** *Dkk1*$^{d/d}$ mice and littermate control (LC) mice were challenged with BLM. On day 14, the lungs were harvested. α-SMA (**A**) and TGF-β1 (**B**) protein levels were analyzed by immunohistochemistry and ImageJ software version 1.52t. **C:** Representative images of immunohistochemistry are shown. A representative of two independent experiments is shown. Data are expressed as means ± SD. $n = 9$ per LC + BLM group (**A** and **B**); $n = 7$ per *Dkk1*$^{d/d}$ + BLM group (**A** and **B**); $n = 5$ per LC group (**A** and **B**); $n = 4$ per *Dkk1*$^{d/d}$ group (**A** and **B**). $^{****}P < 0.0001$ (one-way analysis of variance analyses with Bonferroni's post hoc test). Scale bars: 100 μm (**C**, **top three panel rows**); 20 μm (**C**, **bottom two panel rows**). Original magnification: ×20 (**C**, **top three panel rows**); ×40 (**C**, **bottom two panel rows**). ns, not significant.

the BLM treatment (day −1) and on days 1, 3, 7, 9, and 11, followed by BLM treatment. In the delayed treatment protocol, DKK1 Ab was treated on days 7, 9, and 11 after BLM administration on day 0.

To examine whether neutralization of DKK1 reduces immune cell infiltration in the lung followed by BLM injury, total leukocytes ($CD45^+$) were quantitated by flow cytometry. $CD45^+$ leukocytes were markedly decreased by both treatment protocols (43% and 38% decreases, respectively) (Figure 5B). Consistent with these data, H&E staining showed that both the full treatment and delayed treatment protocols markedly decreased inflammation compared with a positive control group (Figure 5C). An increase in DKK1 protein level was abrogated by both the full treatment and delayed treatment, showing similar basal DKK1 protein levels to the control group (Figure 5D).

Whether neutralization of DKK1 reduces BLM-induced lung fibrosis phenotypes was investigated next. Whether collagen mRNA expression levels and collagen deposition were decreased in the DKK1 Ab−treated group after BLM treatment was examined. Col1a1 mRNA expression levels were decreased in the full treatment group compared with the BLM-treated group (a 68% decrease) (Figure 6A). The delayed treatment groups showed a marked decrease in Col1a1 mRNA expression compared with those receiving BLM treatment alone (a 52% decrease) (Figure 6A).

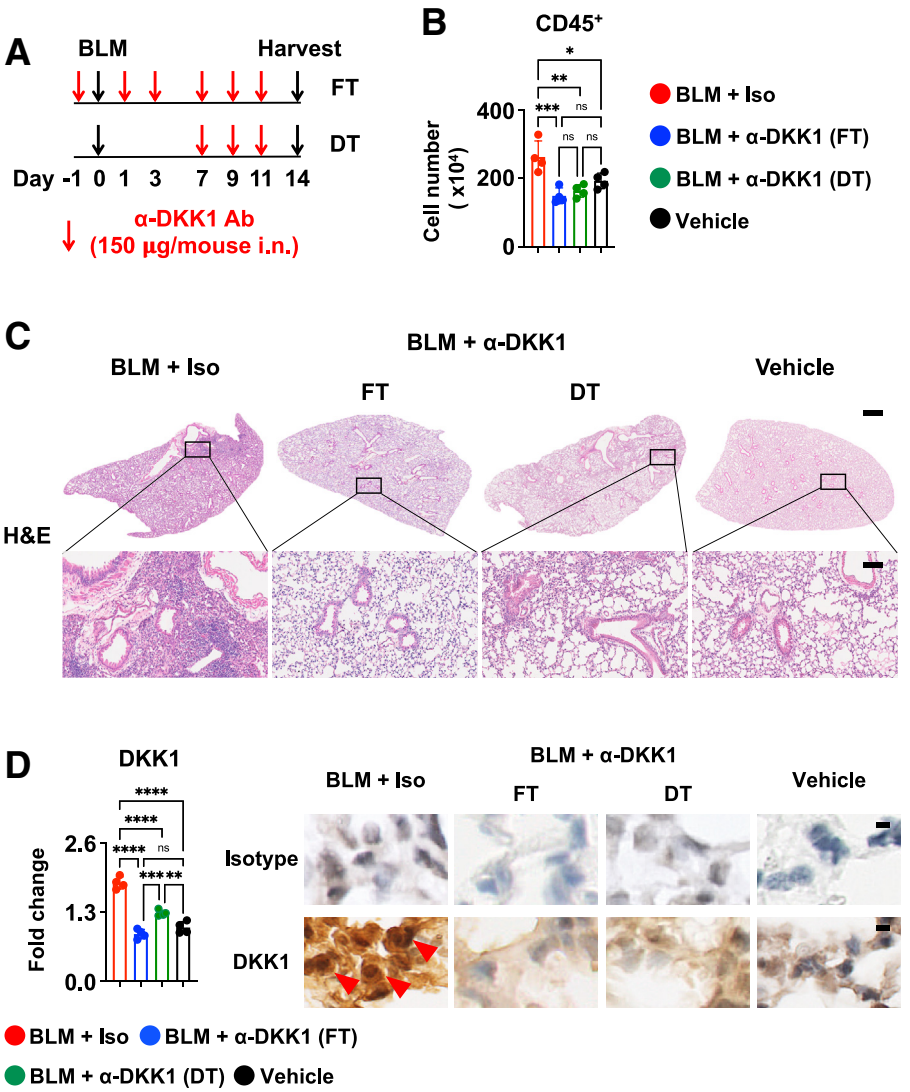

Figure 5 Neutralization of DKK1 reduces bleomycin (BLM)-induced lung inflammation in mice. **A**—**D:** Upon BLM administration, C57Bl/6J mice were challenged with an isotype control antibody (Iso Ab) or anti-DKK1 antibody (α-DKK1 Ab) intranasally. α-DKK1 Ab was treated at the indicated time point (FT, full treatment, DT, delayed treatment) (**A**). **B:** Total leukocytes ($CD45^+$) from lung tissue homogenates were quantitated by flow cytometry. **C:** Representative images of hematoxylin & eosin (H&E) are shown. The **boxed areas** are shown in higher magnification below. **D:** DKK1 protein levels were analyzed by immunohistochemistry and ImageJ software version 1.52t (**left**). Representative images of immunohistochemistry are shown (**right**). DKK1-positive cells are indicated by **arrowheads**. A representative of two independent experiments is shown. Data are expressed as means ± SD. $n = 4$ per group (**B** and **D**). $^*P < 0.05$, $^{**}P < 0.005$, $^{***}P < 0.001$, and $^{****}P < 0.0001$ (one-way analysis of variance analyses with Bonferroni's post hoc test). Scale bars: 800 μm (**C**, **top panels**); 100 μm (**C**, **bottom panels**); 5 μm (**D**). Original magnification: ×1 (**C**, **top panels**); ×10 (**C**, **bottom panels**); ×80 (**D**). ns, not significant.

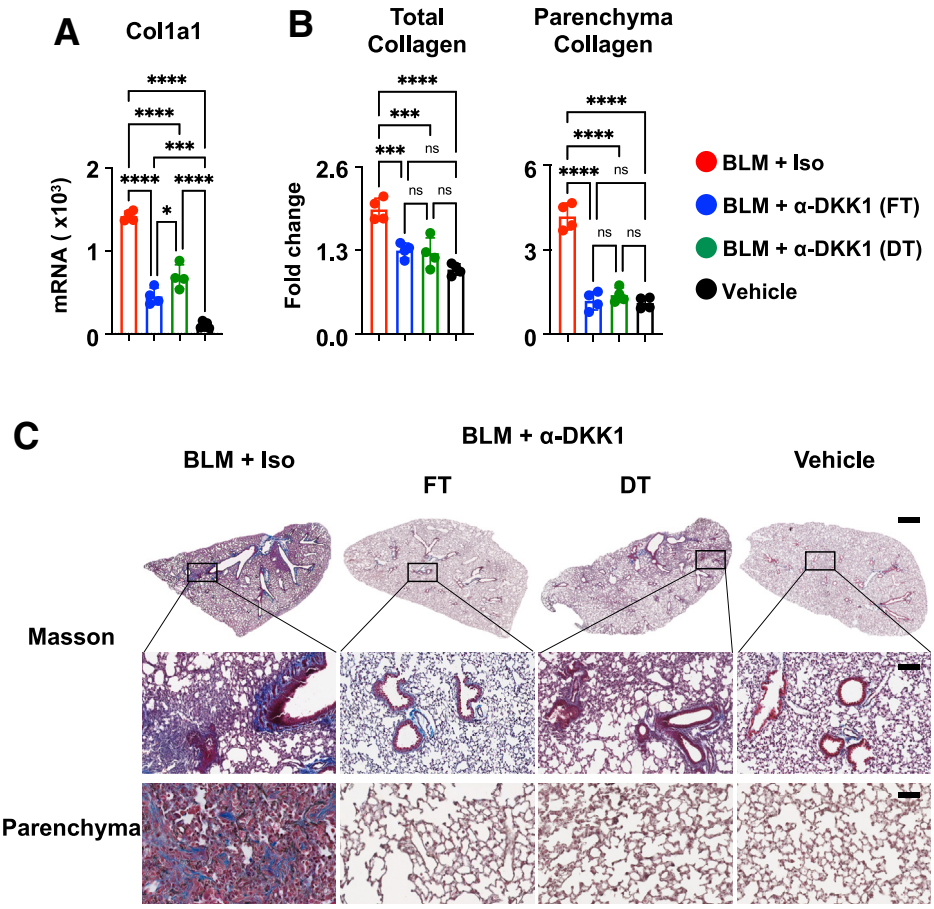

Figure 6 Neutralization of DKK1 reduces collagen deposition upon bleomycin (BLM) challenge. **A**–**C:** Upon BLM administration, C57Bl/6J mice were challenged with anti-DKK1 antibody (α-DKK1 Ab) intranasally (FT, full treatment, DT, delayed treatment). **A:** Lung tissue sections were analyzed by formalin-fixed paraffin-embedded quantitative PCR. Relative Col1a1 gene expression levels were quantitated. **B:** Total collagen and parenchyma collagen deposition were determined by Masson staining and ImageJ software version 1.52t. **C:** Representative images of Masson staining are shown. The **boxed areas** are shown in higher magnification below. A representative of two independent experiments is shown. Data are expressed as means ± SD. $n = 4$ per group (**A** and **B**). $^{*}P < 0.05$, $^{***}P < 0.001$, and $^{****}P < 0.0001$ (one-way analysis of variance analyses with Bonferroni's post hoc test). Scale bars: 800 μm (**C**, **top panels**); 100 μm (**C**, **middle panels**); 20 μm (**C**, **bottom panels**). Original magnification: ×1 (**C**, **top panels**); ×10 (**C**, **middle panels**); ×40 (**C**, **bottom panels**). Iso, isotype; ns, not significant.

Notably, the collagen-positive area in the entire lung tissue sections was decreased by neutralizing DKK1 utilizing either the full treatment (a 35% decrease) or the delayed treatment protocol (a 37% decrease) (Figure 6, B and C). The full treatment and delayed treatment groups showed a more prominent decrease in collagen deposition in the lung parenchyma areas (75% and 72% decreases, respectively) (Figure 6, B and C).

The increased α-SMA mRNA and protein levels were decreased by both the full treatment (49% and 57% decreases, respectively) and delayed treatment protocols (48% and 30% decreases, respectively) compared with the control group (Figure 7, A and C). TGF-β1 mRNA and protein levels were decreased in both Ab treatment protocols [43% and 32% decreases (full treatment) and 50% and 42% decreases (delayed treatment), respectively] (Figure 7, B and D). This indicates that the delayed functional inhibition of DKK1 is comparable to the full treatment protocol to inhibit inflammation and profibrotic phenotypes. These results suggest that DKK1 neutralization can be used as a therapeutic approach in the BLM-induced lung injury and fibrosis model.

Discussion

This study showed that DKK1 promotes lung inflammation and fibrosis phenotypes in the BLM mouse model. The marked decrease in inflammation and fibrosis phenotypes of *doubleridge* mice using the BLM model suggests a proinflammatory role of DKK1 in PF. Neutralization of DKK1 resulted in a substantial decrease in BLM-induced lung fibrosis phenotypes.

The increased DKK1 protein expression of PF patients has been reported.[18] An earlier review and a previous study suggested that DKK1 could play a role as an immune

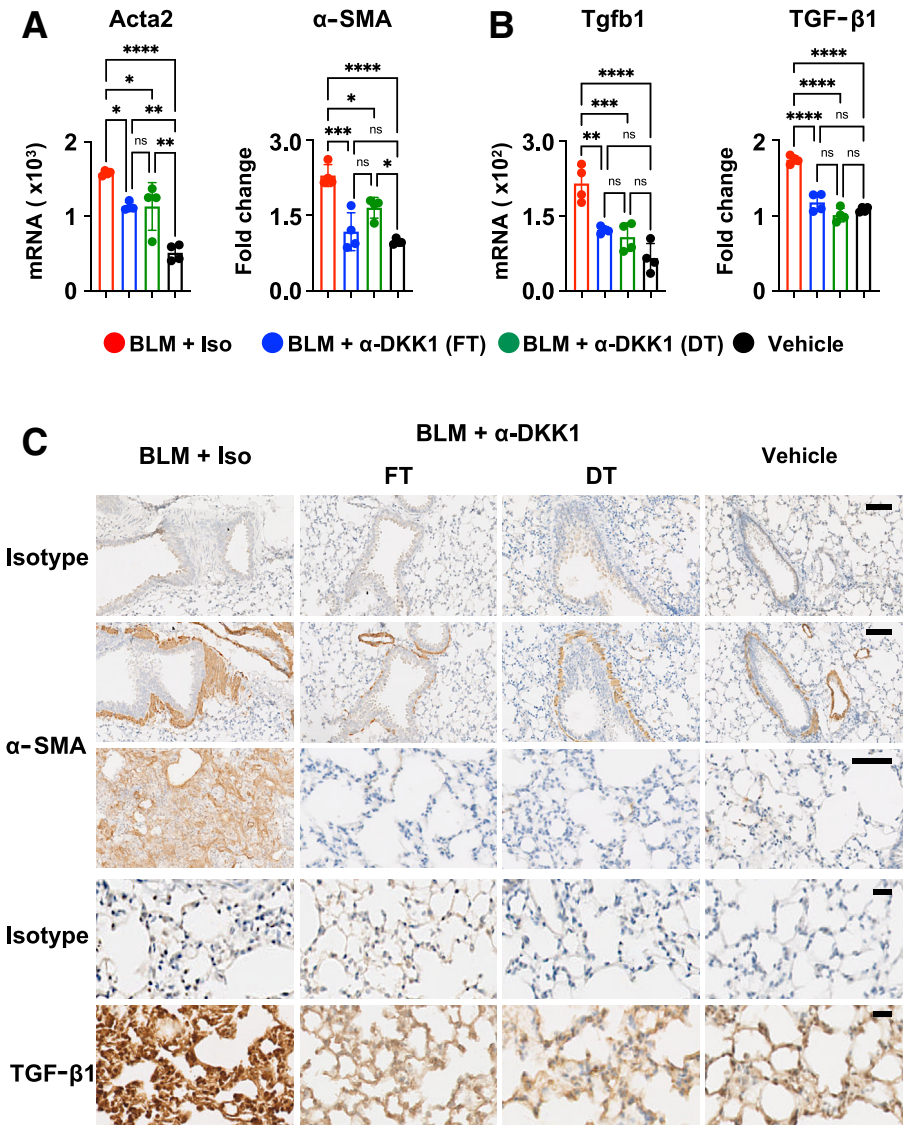

Figure 7 Neutralization of DKK1 reduces bleomycin (BLM)-induced lung fibrosis phenotypes in mice. **A**–**C:** Upon BLM administration, C57Bl/6J mice were challenged with intranasally anti-DKK1 antibody (α-DKK1 Ab) (FT, full treatment, DT, delayed treatment). **A** and **B:** Lung tissue sections were analyzed by formalin-fixed paraffin-embedded quantitative PCR. Relative Acta2 (**A**) and Tgfb1 (**B**) gene expression levels were quantitated. α-SMA (**A**) and TGF-β1 (**B**) protein levels were analyzed by immunohistochemistry and ImageJ software version 1.52t. **C:** Representative images of α-SMA and TGF-β1 immunohistochemistry are shown. A representative of two independent experiments is shown. Data are expressed as means ± SD. $n = 4$ per group (**A** and **B**). $^{*}P < 0.05$, $^{**}P < 0.005$, $^{***}P < 0.001$, and $^{****}P < 0.0001$ (one-way analysis of variance analyses with Bonferroni's post hoc test). Scale bars: 100 μm (**C**, **top three panel rows**); 20 μm (**C**, **bottom two panel rows**). Original magnification: ×20 (**C**, **top three panel rows**); ×40 (**C**, **bottom two panel rows**). ns, not significant.

modulator.[8,30] Yet, the role of DKK1 in PF has remained elusive. This study is the first to demonstrate that reduced expression of DKK1 in *doubleridge* mice protected the host from BLM-induced lung injury with reduced inflammation and fibrosis phenotypes. The little difference between *doubleridge* mice and their littermate control mice in various parameters such as lung immune cell population and histological analyses at steady state suggests that elevated local and systemic levels of DKK1 are required in the inflammation process upon lung injury rather than during homeostasis. Given that other DKKs were elevated in PF patients and they share partial amino acid homology mainly in the colipase fold domain and two conserved cysteine-rich domains, it would be worth studying the role of other DKKs in pulmonary fibrosis.[18,31]

Several studies demonstrated that DKK1 is employed as an important pathological immunomodulator in various inflammatory disease models caused by allergens, infectious pathogens, stromal cells, or tumors cells in cancer.[8,9,32–34] The current study suggests that sterile injury-mediated inflammation such as that caused by bleomycin can also be promoted by DKK1. Notably, the BLM lung injury and fibrosis model showed collagen deposition, revealing that high levels of DKK1 coincided with collagen deposition.

Thus, the proinflammatory and profibrotic role of DKK1 in this study warrants further questions regarding how DKK1-mediated inflammation can be regulated in the BLM-injury model. Further investigation on other murine pulmonary fibrosis models is warranted, given that the BLM model resembles human PF partially. The reduced collagen deposition, along with the reduction of myofibroblast marker α-SMA and profibrotic cytokine TGF-β1, raises interesting questions about whether DKK1 is involved in TGF-β–driven lung fibrosis, given that the role of DKK1 in tissue repair and fibrosis process remained largely unanswered.

The current study results with DKK1 Ab treatment from day −1 (full treatment) were consistent with the BLM-injury model using *doubleridge* mice in that both inflammation and fibrosis phenotypes were reduced by DKK1 Ab treatment. Interestingly, DKK1 Ab administration in ongoing BLM-mediated lung inflammation and fibrosis starting at day 7 showed a comparable inhibition effect to the full treatment from day −1 in the BLM model. This suggests that DKK1 Ab can be used to target PF, indicating that inflammation-induced fibrosis can be inhibited during the BLM model. Two drugs, pirfenidone and nintedanib, have been approved by the US Food and Drug Administration to delay PF. The current results suggest the possibility of using DKK1 Ab with pirfenidone or nintedanib as a combination therapeutic strategy to treat a bigger pool of PF patients. Further studies are warranted to test this combination therapeutic potential. The current study provides a potential inhibition of progressive PF with using DKK1 neutralization in the BLM model. Whether DKK1 Ab treatment will benefit PF patients with established PF without inflammation remains to be investigated.

Taken together, the current study identifies DKK1 as a proinflammatory ligand to promote the BLM-induced lung fibrosis model, placing DKK1 as an attractive molecular target to regulate inflammation-induced fibrosis.

Acknowledgments

We thank Carla Rothlin (Yale), Diane McMahon-Pratt (Yale, retired), and Patty Lee (Duke) for reviewing the manuscript.

Author Contributions

E-A.S. and W-J.C. analyzed the data and wrote the manuscript; E-A.S. and M.H.P. performed experiments; O.H. provided input for qPCR experiments; P.J.S. provided technical input about pulmonary fibrosis; and W-J.C. supervised all aspects of the project. All authors read and revised the manuscript.

Supplemental Data

Supplemental material for this article can be found at *http://doi.org/10.1016/j.ajpath.2023.05.009*.

References

1. Mack M: Inflammation and fibrosis. Matrix Biol 2018, 68-69: 106−121
2. Wynn TA: Integrating mechanisms of pulmonary fibrosis. J Exp Med 2011, 208:1339−1350
3. Whyte JL, Smith AA, Helms JA: Wnt signaling and injury repair. Cold Spring Harb Perspect Biol 2012, 4:a008078
4. Nusse R, Clevers H: Wnt/beta-catenin signaling, disease, and emerging therapeutic modalities. Cell 2017, 169:985−999
5. Jaschke N, Hofbauer LC, Göbel A, Rachner TD: Evolving functions of Dickkopf-1 in cancer and immunity. Cancer Lett 2020, 482:1−7
6. Chae W-J, Bothwell ALM: Dickkopf1: an immunomodulatory ligand and Wnt antagonist in pathological inflammation. Differentiation 2019, 108:33−39
7. Klavdianou K, Liossis S-N, Daoussis D: Dkk1: a key molecule in joint remodelling and fibrosis. Mediterr J Rheumatol 2017, 28: 174−182
8. Chae W-J, Ehrlich AK, Chan PY, Teixeira AM, Henegariu O, Hao L, Shin JH, Park J-H, Tang WH, Kim S-T, Maher SE, Goldsmith-Pestana K, Shan P, Hwa J, Lee PJ, Krause DS, Rothlin CV, McMahon-Pratt D, Bothwell ALM: The Wnt antagonist Dickkopf-1 promotes pathological type 2 cell-mediated inflammation. Immunity 2016, 44:246−258
9. Wu Y, Zeng Z, Guo Y, Song L, Weatherhead JE, Huang X, Zeng Y, Bimler L, Chang C-Y, Knight JM, Valladolid C, Sun H, Cruz MA, Hube B, Naglik JR, Luong AU, Kheradmand F, Corry DB: Candida albicans elicits protective allergic responses via platelet mediated T helper 2 and T helper 17 cell polarization. Immunity 2021, 54: 2595−2610.e7
10. Puttur F, Gregory LG, Lloyd CM: Airway macrophages as the guardians of tissue repair in the lung. Immunol Cell Biol 2019, 97: 246−257
11. Shenderov K, Collins SL, Powell JD, Horton MR: Immune dysregulation as a driver of idiopathic pulmonary fibrosis. J Clin Invest 2021, 131:e143226
12. Richeldi L, Collard HR, Jones MG: Idiopathic pulmonary fibrosis. Lancet 2017, 389:1941−1952
13. Kotsiou OS, Gourgoulianis KI, Zarogiannis SG: IL-33/ST2 axis in organ fibrosis. Front Immunol 2018, 9:2432
14. Li D, Guabiraba R, Besnard A-G, Komai-Koma M, Jabir MS, Zhang L, Graham GJ, Kurowska-Stolarska M, Liew FY, McSharry C, Xu D: IL-33 promotes ST2-dependent lung fibrosis by the induction of alternatively activated macrophages and innate lymphoid cells in mice. J Allergy Clin Immunol 2014, 134:1422−1432.e11
15. Taparra K, Liu H, Polley M-Y, Ristow K, Habermann TM, Ansell SM: Bleomycin use in the treatment of Hodgkin lymphoma (HL): toxicity and outcomes in the modern era. Leuk Lymphoma 2020, 61:298−308
16. Williamson JD, Sadofsky LR, Hart SP: The pathogenesis of bleomycin-induced lung injury in animals and its applicability to human idiopathic pulmonary fibrosis. Exp Lung Res 2015, 41:57−73
17. Aumiller V, Balsara N, Wilhelm J, Gunther A, Königshoff M: WNT/beta-catenin signaling induces IL-1beta expression by alveolar epithelial cells in pulmonary fibrosis. Am J Respir Cell Mol Biol 2013, 49:96−104
18. Pfaff E-M, Becker S, Günther A, Königshoff M: Dickkopf proteins influence lung epithelial cell proliferation in idiopathic pulmonary fibrosis. Eur Respir J 2011, 37:79−87

19. Meizlish ML, Franklin RA, Zhou X, Medzhitov R: Tissue homeostasis and inflammation. Annu Rev Immunol 2021, 39:557−581
20. Jiang D, Dey T, Liu G: Recent developments in the pathobiology of lung myofibroblasts. Expert Rev Respir Med 2021, 15: 239−247
21. Sime PJ, Xing Z, Graham FL, Csaky KG, Gauldie J: Adenovector-mediated gene transfer of active transforming growth factor-beta1 induces prolonged severe fibrosis in rat lung. J Clin Invest 1997, 100:768−776
22. Giri SN, Hyde DM, Hollinger MA: Effect of antibody to transforming growth factor beta on bleomycin induced accumulation of lung collagen in mice. Thorax 1993, 48:959−966
23. Zhao J, Shi W, Wang Y-L, Chen H, Bringas P Jr, Datto MB, Frederick JP, Wang X-F, Warburton D: Smad3 deficiency attenuates bleomycin-induced pulmonary fibrosis in mice. Am J Physiol Lung Cell Mol Physiol 2002, 282:L585−L593
24. Wynn TA: Cellular and molecular mechanisms of fibrosis. J Pathol 2008, 214:199−210
25. Wynn TA, Ramalingam TR: Mechanisms of fibrosis: therapeutic translation for fibrotic disease. Nat Med 2012, 18:1028−1040
26. MacDonald BT, Adamska M, Meisler MH: Hypomorphic expression of Dkk1 in the doubleridge mouse: dose dependence and compensatory interactions with Lrp6. Development 2004, 131: 2543−2552
27. Burgstaller G, Oehrle B, Gerckens M, White ES, Schiller HB, Eickelberg O: The instructive extracellular matrix of the lung: basic composition and alterations in chronic lung disease. Eur Respir J 2017, 50:1601805
28. Ucero AC, Bakiri L, Roediger B, Suzuki M, Jimenez M, Mandal P, Braghetta P, Bonaldo P, Paz-Ares L, Fustero-Torre C, Ximenez-Embun P, Hernandez AI, Megias D, Wagner EF: Fra-2-expressing macrophages promote lung fibrosis in mice. J Clin Invest 2019, 129:3293−3309
29. Izbicki G, Segel MJ, Christensen TG, Conner MW, Breuer R: Time course of bleomycin-induced lung fibrosis. Int J Exp Pathol 2002, 83: 111−119
30. Gieseck RL 3rd, Wilson MS, Wynn TA: Type 2 immunity in tissue repair and fibrosis. Nat Rev Immunol 2018, 18:62−76
31. Niehrs C: Function and biological roles of the Dickkopf family of Wnt modulators. Oncogene 2006, 25:7469−7481
32. Guo Y, Mishra A, Howland E, Zhao C, Shukla D, Weng T, Liu L: Platelet-derived Wnt antagonist Dickkopf-1 is implicated in ICAM-1/VCAM-1-mediated neutrophilic acute lung inflammation. Blood 2015, 126:2220−2229
33. D'Amico L, Mahajan S, Capietto AH, Yang Z, Zamani A, Ricci B, Bumpass DB, Meyer M, Su X, Wang-Gillam A, Weilbaecher K, Stewart SA, DeNardo DG, Faccio R: Dickkopf-related protein 1 (Dkk1) regulates the accumulation and function of myeloid derived suppressor cells in cancer. J Exp Med 2016, 213:827−840
34. Malladi S, Macalinao DG, Jin X, He L, Basnet H, Zou Y, de Stanchina E, Massagué J: Metastatic latency and immune evasion through autocrine inhibition of WNT. Cell 2016, 165:45−60